An application of the J-integral engineering approach to blunt notch specimens

R. ROBERTI and A. GHIDINI, Dipartimento di Chimica-Fisica Applicata, Politecnico di Milano, Milan, Italy.
D. FIRRAO, Dipartimento di Scienza dei Materiali e Ingegneria Chimica, Politecnico di Torino, Turin, Italy.

Abstract

The influence of notch root radius on crack growth resistance behaviour (J-Resistance curve) of a C-Mn structural steel was investigated by fracture mechanics experiments with three-point bending specimens. J-R Curves was determined by the multiple specimen technique and it was found that, while the J-integral at initiation is differently affected by small and large notch root radii, the tearing modulus, on the contrary, is independent on notch root radius.
The J-R curves have also been obtained by applying the estimation scheme developed by Kumar, German and Shih to evaluate the crack driving force; the estimation scheme was also utilized to evaluate the loading behaviour of both cracked and blunt notched specimens.
The comparison between predictions and experimental results has generally shown a good accordance, thus extending the applicability of the J-integral engineering approach to blunt notch specimens.

Riassunto

Applicazione a campioni con intaglio non acuto del metodo ingegneristico di calcolo dell'integrale J

È stata studiata l'influenza del raggio di fondo intaglio sulla resistenza alla propagazione di cricca (curva J-R) di un acciaio di costruzione al C-Mn, mediante prove di meccanica della frattura su provini di flessione su tre punti. Le curve J-R sono state determinate mediante la metodologia multiprovino ed è stato trovato che mentre il valore dell'integrale J all'innesco della propagazione è influenzato dal raggio di fondo intaglio, la pendenza delle curve J-R risulta costante al variare del raggio di fondo intaglio medesimo. Le curve J-R sono state anche ottenute facendo uso della procedura sviluppata da Kumar, German e Shih per la previsione della « forza spingente » per la propagazione della cricca; tale procedura è stata anche applicata con lo scopo opposto di stimare il comportamento sotto carico crescente dei provini di flessione su tre punti impiegati.
Il confronto fra le previsioni ed i risultati sperimentali ha in generale messo in evidenza un buon accordo, consentendo di concludere affermativamente circa la possibilità di estensione dell'applicabilità dell'approccio ingegneristico dell'integrale J ai campioni ed alle strutture contenenti difetti con un raggio di fondo intaglio finito.

Introduction

Crack driving force diagrams, derived according to the procedure of the J-integral engineering approach to fracture analysis developed by Kumar, German and Shih,[1-3] are a well recognized useful tool to analyze crack growth initiation and propagation in a cracked body, provided that fully plastic solutions are available for the specific geometry of interest and that the material's true stress-true strain curve can be approximated by the Ramberg-Osgood law.
The procedure to estimate the elastic-plastic solutions consists of an interpolation by simple summation between the elastic solutions and the fully plastic solutions. The elastic solutions are obtained by converting to J-integral the solutions for the stress intensity factor reported in the Linear Elastic Fracture Mechanics handbooks, by means of the usual formula $J = K^2/E'$ ($E' = E$ for plane stress and $E' = E/(1 - \nu^2)$ for plane strain); the fully plastic solutions are generally expressed as reported in the following formula:

$$J = \alpha\, \sigma_Y\, \varepsilon_Y\, c\, h_1\, (P/P_o)^{(n+1)} \qquad (1)$$

where P is the applied load, P_o the limit load, σ_Y the yield stress, ε_Y the yield strain, c = W/a the uncracked ligament, h_1 a dimensionless quantity function of a/W and n; α and n are the coefficients in the Ramberg-Osgood law:

$$\varepsilon/\varepsilon_o = \alpha\, (\sigma/\sigma_o)^n \qquad (2)$$

Equations similar to (1) were also developed to obtain fully plastic solutions for the load point displacement Δ or the crack mouth opening δ.
The crack driving force diagram consists of a plot of the elastic-plastic estimated J-integral versus crack length, with the applied load and the load point displacement as the parameters. The comparison between the J-integral crack driving force and the material's J-Resistance (J-R) curve allows to perform a complete analysis of the ductile fracture process by predicting various quantities such as the load at crack initiation, the maximum load carrying capacity, the load-displacement behaviour, the extent of stable crack growth prior to instability.
In fact, as shown in Fig. 1, where a schematic crack driving force diagram is reported, the constant load curve intersecting the J-R curve at the J_{Ic} value gives the load at the onset of crack initiation, while the tangency of a constant load curve and the J-R curve gives the maximum attainable load during crack growth.

Fig. 1 - Scheme of a crack driving force diagram. The constant load curves are shown by solid lines, and the constant displacement curves by dashed lines (3).

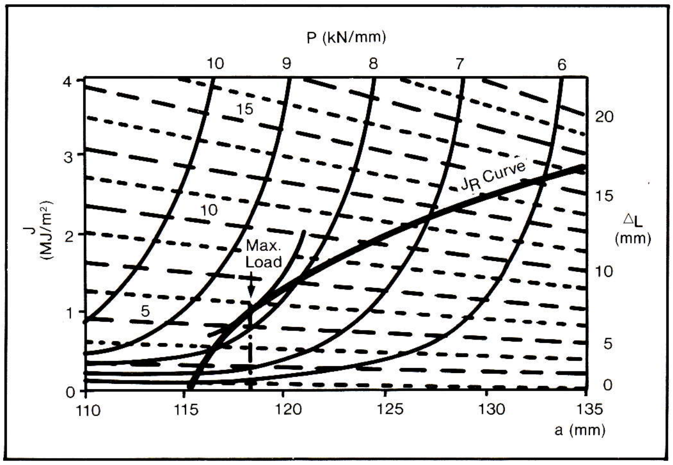

Furthermore, considering that the conditions for equilibrium of crack growth are obtained when the applied crack driving force in terms of J-integral equals the material's resistance to crack growth, then the intersection of a constant load curve and a constant load point displacement curve at a point on the J-R curve yields the respective values of load and displacement in equilibrium at the corresponding crack length. Therefore the full load displacement behaviour of the cracked body can be predicted.
The construction of the crack driving force diagram, besides the prediction of the load-load line displacement of the flawed structure from the experimentally determined material's J-R curve, allows also the opposite application, namely the prediction of J-R curve from a single load-load point displacement curve of the cracked structure under test.
Both applications of the engineering approach have been tried with adverse results.[4-8] However, it is generally agreed that the accuracy of the prediction is firstly dependent on the capability of the Ramberg-Osgood law to describe the material's true stress-true strain behaviour. Furthermore, the major discrepancies between the prediction and the experimental behaviour have been found when the estimation scheme is used to predict the J-R curve from the load-load line displacement behaviour of the cracked structure under test.
Fully plastic solutions have been reported for a number of common structural configurations and in particular for fracture mechanics standard specimen geometries.[3] Therefore, as a particularly interesting application, the J-integral engineering approach is represented by the possibility of obtaining a J-R curve from a single specimen test.
In the present paper, the J-integral estimation scheme has been applied to C-Mn structural steel three-point bending specimens, both pre-cracked or containing a notch with a finite root radius instead of the fatigue pre-crack. J-R curves predicted by means of the estimation scheme have been compared with the experimental ones, obtained by the multiple specimen technique; the comparison between the predicted and experimental load-displacement behaviour has also been performed.

Experimental procedure

Tensile and fracture mechanics tests have been carried out by means of a 100 kN screw-driven Instron 1195 machine.
The notch root radii ρ of the three-point bending specimens had been chosen, according to previous results on similar steels,[9] equal to 0 (fatigue pre-crack), 0.05 and 0.25 mm. Experimental J-R curves have been obtained by means of the multiple specimen technique, according to the ASTM E813-81 Standard.
The application of the J-integral estimation scheme has been performed in accordance to the procedure described by Kumar, German and Shih[3] using the J-integral and load point displacement plane strain fully plastic solutions for the three-point bending geometry.

Results and discussion

The room temperature mechanical properties of the C-Mn steel are reported in Table 1, along with the coefficients of the Ramberg-Osgood equation. The Table also reports the steel chemical composition. The true stress-true strain experimental curve of a tensile specimen, together with the Ramberg-Osgood fit are reported in Fig. 2; a very good accordance between them can be observed.
The J-R curves for the three notch root radii are reported in Fig. 3. The blunting line applies only to the J-R curve of the fatigue pre-cracked specimens, as blunting has no meaningful effect in producing fictitious crack advancement in blunt notch specimens; therefore, for the latter specimens the J-R curves are

TABLE 1 - Composition (wt. pct.), mechanical properties and coefficients of the Ramberg-Osgood law (equation 2) pertaining to the steel employed

C	Mn	Si	P	S	
0.155	1.36	0.23	0.010	0.012	
YS (MPa)	UTS (MPa)	ε_y	e_f (%)	n	α
348	510	0.00687	30.4	5.38	1.04

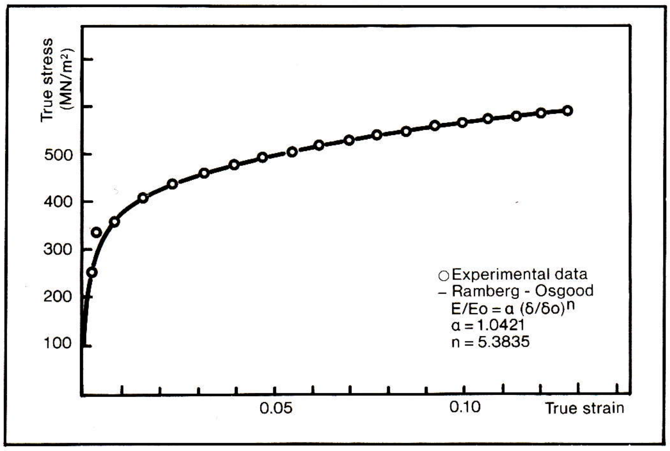

Fig. 2 - True stress-true strain curve of the C-Mn steel.

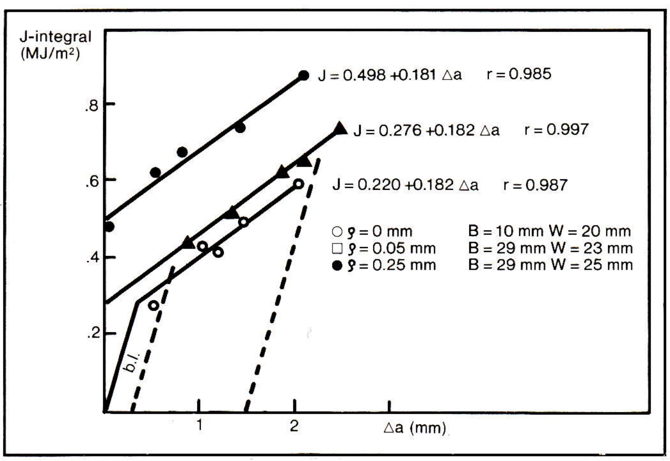

Fig. 3 - J-Resistance curves of the C-Mn steel (ASTM E 813-81, multiple test-pieces) for three-point bending specimens with different notch root radius (ρ), thickness (B) and width (W); b.l. is the blunting line of equation $J = (\sigma_y + \sigma_u) \cdot \Delta a$

extrapolated to the ordinate axis.

From the J-R curves it can be seen that the resistance to crack advancement is the same at varying notch root radii, as the slope dJ/da is constant and independent on the applied J-integral level.

On the contrary, the J-integral applied at initiation is dependent on the notch root radius: a more detailed discussion on the existence of an effective notch root radius (behaving like a fatigue pre-crack) and its relationship with the microstructural parameters has been performed by the authors and has been reported elsewhere.[10-12]

In addition, it must be observed that crack advancement has been extended well besides the limit which ensures that the fracture process zone is included in the region of dominance of the Hutchinson, Rice and Rosengren's field.[13-14] Nevertheless, the J-R curves have a constant slope in the whole range of experimented crack advancements, and therefore the

Fig. 4 - Crack driving force diagram for a plane strain three-point bending specimen of a C-Mn steel, with a notch root radius $\rho = 0$ mm (B = 10 mm, W = 20 mm, initial notch length, $a_o = 10.6$ mm).

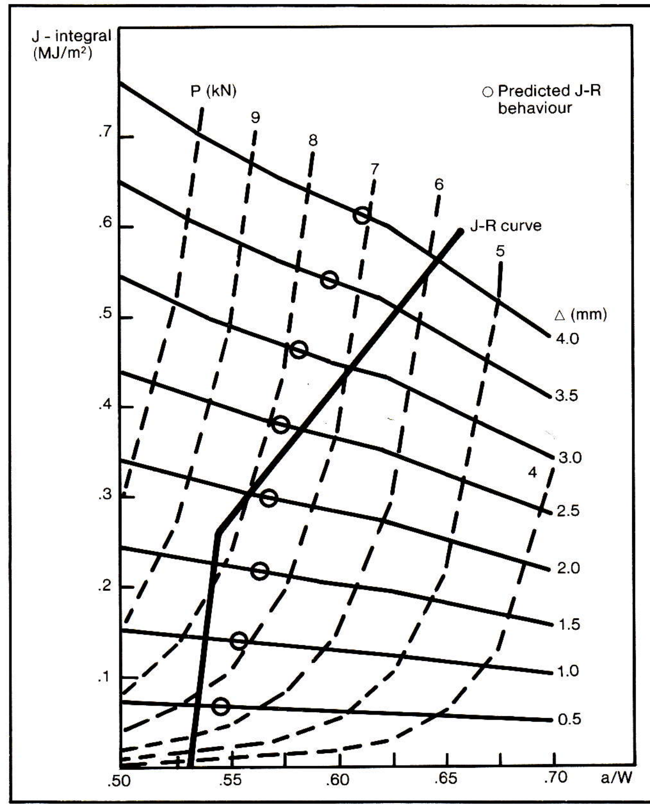

Fig. 5 - Crack driving force diagram for a plane strain three-point bending specimen of a C-Mn steel, with a notch root radius $\rho = 0.05$ mm (B = 29 mm, W = 23 mm, initial notch length, $a_o = 11.5$ mm).

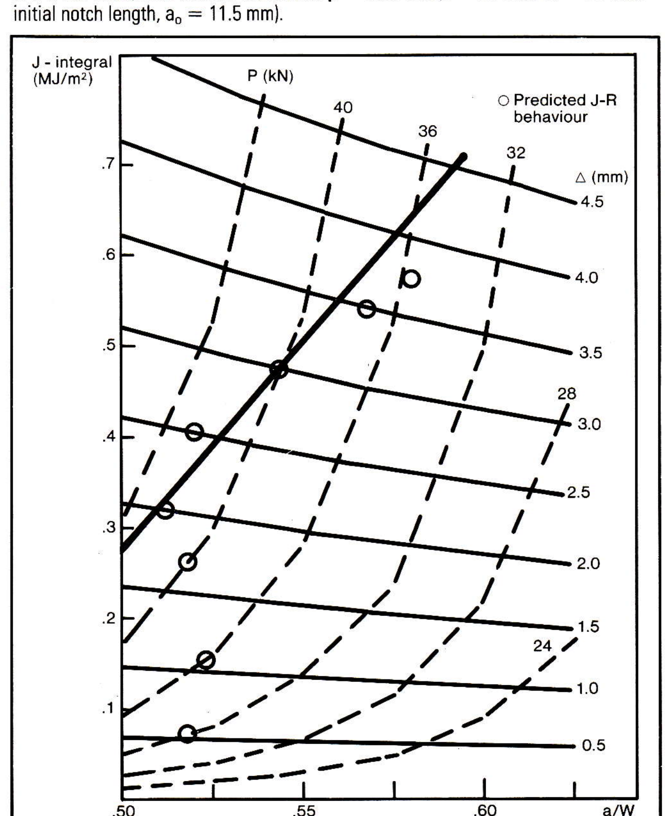

J-integral seems to be applicable as a crack tip characterizing parameter also besides the previously mentioned limits.
The crack driving force diagrams for the specimens with different notch root radii are reported in Figs. 4, 5 and 6.
First of all, it must be remembered that in the original estimation scheme [1-3] only cracked specimens or bodies are considered; however, since the procedure of application doesn't discriminate the case of a cracked body from the one of a body with a finite notch root radius defect, the crack driving force diagrams that have been obtained for blunt notch specimens (Figs. 5 and 6) are the same as for cracked specimens having equal sizes and crack length-to-width ratio. On the crack driving force diagrams, there are, superimposed, the experimental J-R curves (heavier solid lines) at the appropriate crack length or notch depth, while the predicted J-R curves are represented by the points, corresponding to couples of load P and load point displacement Δ values of the experimental loading curve related to the pertaining specimen.

Fig. 6 - Crack driving force diagram for a plane strain three-point bending specimen of a C-Mn steel, with a notch root radius $\rho = 0.25$ mm (B = 29 mm, W = 25 mm, initial notch length, $a_o = 12.5$ mm).

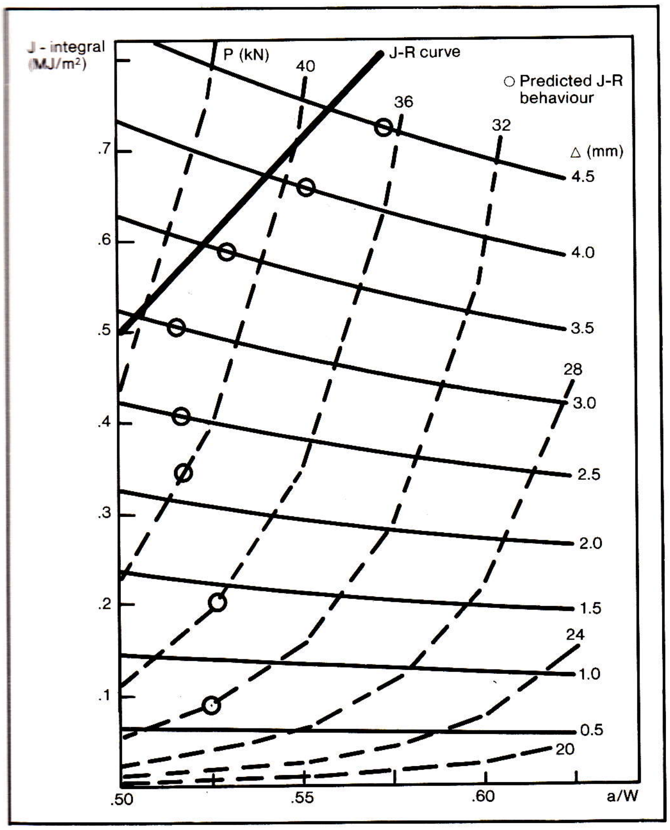

The agreement between the experimental J-R curves and the predicted ones is, in general, good enough. Such an agreement is much better if the J-R curves of blunt notched specimens are considered. In fact, both the initial part of the J-R curve before the onset of crack propagation, when the J integral rises at constant notch depth, and the second part, corresponding to the J resistance to crack advancement (dJ/da = constant) are fairly well predicted and also the intersection between the two parts of the J-R curves, that is the J value at crack initiation from the notch root, is in good agreement with the experimental one.
Figs. 7 through 9 show the comparison between the experimental and the estimated load-load line displacement (P-Δ) curves of the three-point bending

Fig. 7 - Comparison between the experimental and the estimated load-load line displacement curves of a plane strain three-point bending specimen of a C-Mn steel, with a notch root radius $\rho = 0$ mm.

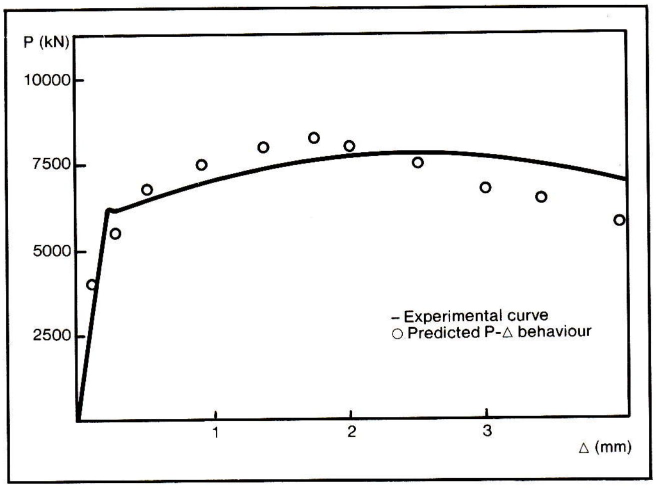

Fig. 8 - Comparison between the experimental and the estimated load-load line displacement curves of a plane strain three-point bending specimen of a C-Mn steel, with a notch root radius $\rho = 0.05$ mm.

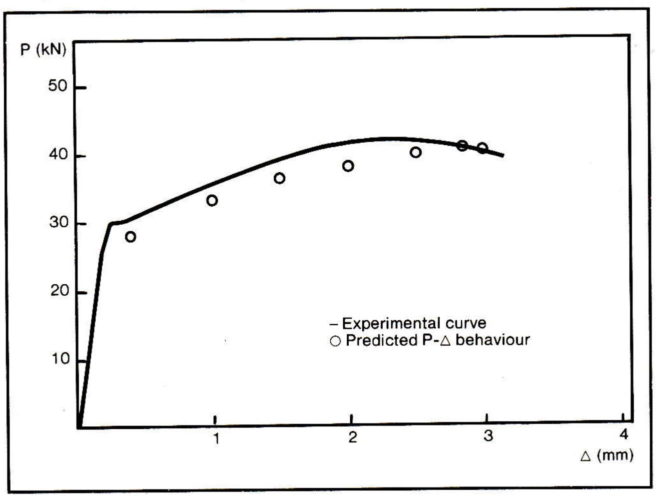

specimens with different notch root radii. From the diagrams, one can see that the estimation scheme allows a good prediction of the loading behaviour of both the pre-cracked specimens and the ones with a finite notch root radius; in particular the predicted load levels are in very good accordance with the experimental ones, while a rather high disagreement is presented between the load line displacements at the maximum load.

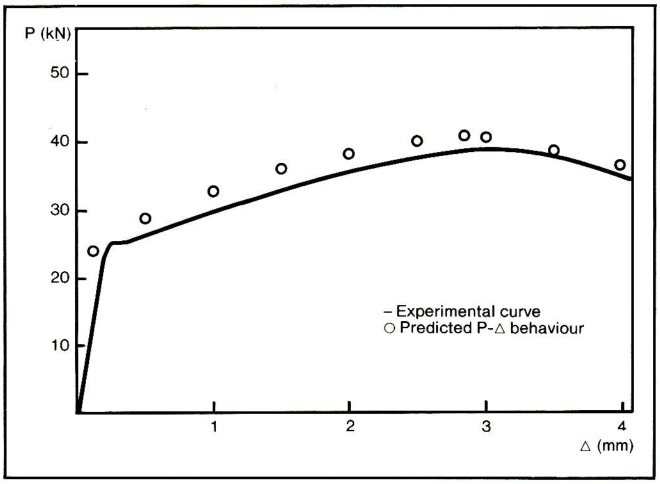

Fig. 9 - Comparison between the experimental and the estimated load-load line displacement curves of a plane strain three-point bending specimen of a C-Mn steel, with a notch root radius $\rho = 0.25$ mm.

Conclusions

The evaluation of the failure behaviour of pre-cracked and blunt notched three-point bending specimens using the J-integral engineering approach developed by Kumar, German and Shih allows to conclude that the use of the estimation scheme can be extended also to specimens with a finite notch root radius, both to predict the load-load line displacement behaviour or to obtain the J-Resistance curve from a single loading curve.
Although a good accordance between predictions and experimental results has been in general obtained, in particular it seems that the accuracy of the method in the case of pre-cracked specimens is fairly good only.

REFERENCES

(1) Shih, C.F., and V. Kumar. Estimation technique for the prediction of elastic-plastic fracture of structural components. ***First Semiannual Report for the EPRI****, Palo Alto, Calif., 1st June 1980.*

(2) Kumar, V., and C.F. Shih. Fully plastic crack solutions, estimation scheme, and stability analyses for the compact specimen. ***Fracture Mechanics: Twelfth Conference, ASTM STP 700****. American Society for Testing and Materials, 1980, pp. 406-438.*

(3) Kumar, V., M.D. German, and C.F. Shih. An engineering approach for elastic-plastic fracture analysis. ***EPRI Report NP-1931****, RP 1237-1, July 1981.*

(4) Milne, I. Failure assessment diagrams and J estimates: a comparison for ferritic and austenitic steels. ***Int. J. Press. Vess. & Piping, 13*** *(1983), 107-125.*

(5) Akhurst, K.N., and I. Milne. Failure assessment diagrams and J estimates: validation for an austenitic steel. In G.C. Sih, E. Sommer, W. Dahl (Eds.), ***Application of Fracture Mechanics to Materials and Structures****. Martinus Nijhoff, The Hague, 1984, pp. 401-413.*

(6) Steenkamp, P. Applicability of the EPRI estimation scheme for the prediction of load-load line displacement behaviour and for single specimen J-R curve determination. ***Int. J. of Fracture, 23*** *(1983), r91-r100.*

(7) Rousselier, G. Workshop: The EPRI method. ***Advanced Seminar on Fracture Mechanics*** *(ASFM 4), Ispra, Italy, October 24-28, 1983.*

(8) Hodulak, L., and J.G. Blauel. Application of two approximate methods for ductile failure assessment. ***Elastic-Plastic Fracture: Second Symposium, Volume II - Fracture Resistance Curves and Engineering Applications. ASTM STP 803****. American Society for Testing and Materials, 1983, pp. 103-114.*

(9) Roberti, R., G. Silva, D. Firrao, and B. De Benedetti. Influence of notch root radius on ductile rupture fracture toughness evaluation with Charpy-V type specimens. ***Int. J. Fatigue, 3*** *(1981), 133-141.*

(10) Firrao, D., and R. Roberti. A model for plane strain ductile fracture toughness. In R.C. Gifkins (Ed.), ***Strength of Metals and Alloys****. Pergamon Press, Oxford, 1982, pp. 947-952.*

(11) Firrao, D., and R. Roberti, Sui parametri microstrutturali che controllano la tenacità alla frattura degli acciai. ***La Metall. Ital., 75*** *(1983), 645-651.*

(12) Firrao, D., and R. Roberti. Ductile fracture nucleation ahead of sharp cracks. ***Metallurgical Science and Technology, 1*** *(1983), 5-13.*

(13) Hutchinson, J.W. Plastic stress and strain fields at a crack tip. ***J. Mech. Phys. Solids, 16*** *(1968), 337-347.*

(14) Rice, J.R., and G.F Rosengren. Plane strain deformation near a crack tip in a power-law hardening material. ***J. Mech. Phys. Solids, 16*** *(1968), 1-12.*